International Journal of Hydrogen Energy 242 (2026) 155582

Contents lists available at ScienceDirect

International Journal of Hydrogen Energy

journal homepage: www.elsevier.com/locate/he

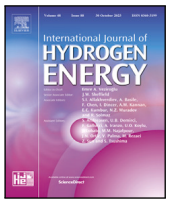

A systematic DFT investigation of hydrogen sorption properties on 3*d*, 4*d* and 5*d* TM-doped Mg(0001) surfaces

M. Pozzo [a,c,*], D. Alfè [b,c]

[a] Faculty of Technological & Innovation Sciences, Department of Engineering and Sciences, Universitas Mercatorum, Piazza Mattei 10, 00186, Rome, Italy
[b] Dipartimento di Fisica Ettore Pancini, Università di Napoli Federico II, Monte S. Angelo, I-80126, Napoli, Italy
[c] Department of Earth Sciences, London Centre for Nanotechnology and Thomas Young Centre@UCL, University College London, Gower Street, London WC1E 6BT, United Kingdom

ARTICLE INFO

Keywords:
Hydrogen storage
Magnesium
Transition metal doping
Density functional theory
d-band centre
Projected density of states

ABSTRACT

The catalytic effect of all 3*d*, 4*d* and 5*d* transition metals (TMs) as possible dopants of a Mg(0001) surface to enhance its hydrogen sorption properties has been systematically studied with Density Functional Theory (DFT). We discuss on-surface adsorption and first three-layer substitutional preferences of all TMs and compare results with those already available in literature. Our findings show that most of them prefer to substitute in the second layer, apart from Cd and Hg preferring the first layer — and from Co, Zn, Ru, Rh, Lu and Au preferring the third layer instead. We also present a compilation of *d*-band centre position values for all the TMs of the Periodic Table. Using this descriptor in the context of the Hammer & Norskov model, we find that Fe, Ni and Rh remain the most active catalysts among all TMs, securing low activation barriers for both hydrogen dissociation and diffusion processes.

1. Introduction

The transition to a green economy solely based on renewable energy sources is a worldwide goal and a yet to be solved challenge. It has been several decades since the scientific community has focused on hydrogen storage as clean energy fuel for mobile applications, its combustion product being simply water (see for example reviews by Møller et al. [1], Shao et al. [2], Sun et al. [3], Abe et al. [4]). Of course, hydrogen needs to be produced from renewable energy resources, but even when this is done a major challenge remains its storage, especially in the context of mobile applications. Among promising candidates for hydrogen storage purposes, magnesium has received much attention due to its natural abundance, high H storage capacity, low cost, lightweight, and cyclability. However, due to a slow kinetics (high energy barriers for hydrogen dissociation and diffusion) and high working temperatures, the hydrogen storage properties of Mg-based materials are yet to be improved for practical transportation purposes (see recent reviews by Yang et al. [5], Hong et al. [6] and Borcholoo & Nekouee [7]).

In previous investigations [8,9] we studied the effect of transition metal (TM) doping on molecular hydrogen dissociation and hydrogen diffusion on a Mg(0001) surface with DFT calculations. Although the diffusion of atomic hydrogen on a pure Mg surface is facile, the presence of a significant energy barrier makes the dissociation of molecular hydrogen difficult, hindering the whole process of forming the hydride. The aim, therefore, is to find a TM able to facilitate the dissociation process, without hindering diffusion. In particular, we investigated most of the 3*d* and 4*d* TMs (Ti, Zr, V, Fe, Ru, Co, Rh, Ni, Pd, Cu, and Ag) apart just a few of them (Cr, Mn, Nb, Mo and Tc). We considered TMs atoms substitutions in the first layer. We showed that the elements to the left of the Periodic Table help with dissociation, reducing the energy barrier, but also make diffusion more difficult, those on the right do not affect H diffusion too much, but they are also less useful in reducing the energy barrier for the dissociation of the hydrogen molecule.

Among all the TMs investigated, we found that Fe, Ni and Rh are the best catalysts, compromising between the energetics of the two different processes. We found that a good descriptor of this activity was the position of the *d*-band centre, according to the Hammer & Nørskov model [10]. From all the results collected, we predicted an expected *d*-band centre value of about −1.29 eV for the ideal dopant of a Mg surface.

At the same time, Banerjee et al. [11] investigated the interaction of molecular hydrogen with pure and TM (Ti, V, and Ni) doped Mg(0001) surfaces using first-principles calculations. They showed that the 3*d* metals Ti, V and Ni prefer to substitute one Mg atom in the second layer, rather than the first. They calculated both dissociation and diffusion barriers and found that whereas dissociation is facilitated

* Corresponding author.
E-mail address: monica.pozzo@unimercatorum.it (M. Pozzo).

https://doi.org/10.1016/j.ijhydene.2026.155582
Received 19 February 2026; Received in revised form 22 April 2026; Accepted 13 May 2026

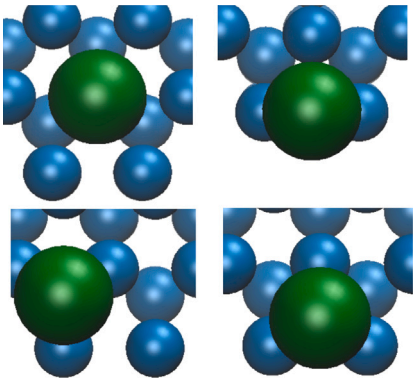

Fig. 1. The four possible adsorption sites investigated for TM adsorption (clockwise: top, bridge, hollow-hcp and hollow-fcc) on a Mg(0001) surface. Colour code is green for the TM atom, light blue for Mg atoms. (For interpretation of the references to colour in this figure legend, the reader is referred to the web version of this article.)

when the TM atoms sit on the surface, diffusion is instead improved when TM atoms are placed in the second layer, because the H atom does not stick too strongly to the TM in a deeper layer.

Soon after, Wu et al. [12] presented DFT results for hydrogen dissociation on a pure and on a Pt-doped Mg(0001) surface. They found that the dissociation process is facilitated when the surface is doped with the 5*d* transition metal, giving an energy barrier of 0.39 eV against 1.05 eV of the pure surface. However, no investigation was carried out for hydrogen diffusion on the Pt-doped Mg surface.

Chen et al. [13] studied the stability of TMs on Mg(0001) surfaces and their effects on H adsorption. They carried out both magnetic and non-magnetic calculations for all the 3*d* and 4*d* TMs (including Sc, Cr, Mn, Zn, Y, Nb, Mo, Tc and Cd which were not studied in our previous works), and for Pt and Au among the 5*d* TMs, as dopants in the first and second layer. They found that spin-polarised calculations are required for Cr, Mn and Fe, but not for Ni and Co. Their results show that all TMs prefer to substitute a Mg atom in the second layer, in line with what previously found by Banerjee et al. [11] for Ti, V and Ni. However, from a close inspection of their Fig. 1, we note a slight preference for Cd to substitute in the first layer instead.

Subsequently, Chen et al. [14] performed a theoretical study of hydrogen dissociation and diffusion on pure, Nb-doped, Ni-doped, and NbNi co-doped Mg(0001) surfaces. Their results show that both Ni and Nb prefer to substitute in the second layer instead of the topmost one. They find that hydrogen dissociation is facilitated when Ni is located in the first layer (in agreement with past literature), however, there is almost no catalytic effect when Ni is located at the energetically favoured second layer. With regard to Nb, the dissociation barrier is reduced at both locations. For both individual Ni and Nb doping, the diffusion barriers are slightly increased with respect to the pure surface. When considered for surface co-doping, whereas the dissociation barrier is significantly reduced, the corresponding diffusion barrier increases with respect to that on the pure Mg surface.

Later on, Wang et al. [15] studied doping with TMs from Sc to Au (all 3*d*, 4*d* and most of 5*d* but no Lu, nor Hg) substituted at first, second and third layer. They reported that spin-polarised calculations must be used for Fe, Ni, and Co. They found that transition metals on the left of the Periodic Table (Sc, Ti, V, Y, Zr, Nb, Hf, Ta and W) prefer to substitute one Mg atom in the second layer, whereas all the other TMs at the centre and right of the Periodic Table (Cr, Mn, Fe, Co, Ni, Cu, Zn, Mo, Tc, Ru, Rh, Pd, Ag, Cd, Re, Os, Ir, Pt and Au) prefer to substitute in the first layer. In addition, they find that Cd, is the only one preferring to be adsorbed on the surface. Finally, Fe turns out to be the best dopant on the Mg surface for molecular hydrogen dissociation.

A few years later, Tang et al. [16] studied all 3*d* and 4*d* TMs, plus Pt and Au as 5*d* TMs substitutions on Mg(0001). They performed spin-polarised calculations in all cases and considered TMs substituted in the first and second layer. Their results show that all TMs prefer to substitute in the second layer, apart from Cd, which prefers to substitute in the first layer.

It has to be noted here that both Chen et al. [13,14] and Tang et al. [16] doped the surface by substituting one Mg atom with a TM atom, as we did in our previous works too, whereas Wang et al. [15] replaced one of the Mg atoms in the first/second/third layer of the Mg(0001) surface with a TM atom while moving the replaced Mg atom on the surface (they mention four different adsorption sites – top, bridge, fcc and hcp – so we guess the most favourable was chosen accordingly) and therefore a comparison of the results with those of Wang et al. would not be meaningful.

Recently, Han et al. [17] studied the location-dependent effect of Ni doping on hydrogen dissociation and diffusion on Mg(0001) by considering first, second and third layer substitutions. Their DFT results are in agreement with previous findings in literature, i.e., Ni prefers to locate inside bulk Mg. However, backed also by their experimental findings, they show that in this case the catalytic effect of Ni on hydrogen dissociation/diffusion is suppressed/undermined. Therefore, they conclude that to take advantage of the catalytic effects of the TM, it is crucial to stabilise Ni atom on the surface or in the topmost layer of Mg(0001).

Wang et al. (2014) reported the position of the *d*-band centres for some of the 3*d* TMs (Zn, Ni, Fe, Co, Mn, V, Ti, Sc; but see our previous comment above) and Han et al. (2022) for Ni. Since the *d*-band centre position is correlated to the height of the activation barriers and a very good descriptor of the reactivity of a metal surface, it seems convenient to build a full inventory of *d*-band centre values for all the 3*d*, 4*d* and 5*d* TMs. As such, it can be used to pinpoint promising systems to follow up with more computationally costly activation barriers calculations.

We therefore decided to extend our previous investigations to cover all 3*d*, 4*d*, and 5*d* TMs of the Periodic Table, from Sc to Hg included, with the aim to search for a possible TM giving a *d*-band centre value close to the ideal value of 1.29 eV we previously highlighted.

Methods used for our systematic investigation are summarised in Section 2. Section 3 summarises our results regarding on-surface adsorption preferential sites, first/second/third layer substitutional preferences and *d*-band centre position values for all the 3*d* to 5*d* TMs here investigated. Conclusions follow in Section 4.

2. Computational method

All the DFT calculations for this work were performed by using similar techniques to those we used in our previous investigations on TM-doped Mg surfaces [8,9]. The simulation package VASP [18] was used with the projector augmented wave (PAW) method [19,20] and the PBE exchange–correlation functional [21]. Details of the PAW potentials are reported in Tables 2–4. In addition, of all the new TMs studied in the present work, only Cr requires spin-polarised calculations, as discussed in Section 3.1. A plane-wave basis set was used to expand the electronic wave-functions with an energy cutoff of 270 eV, in line with our previous works. Adsorption energies calculated with this plane-wave cutoff are converged to better than 10 meV.

Surfaces were modelled using periodic slabs, with 5 atomic layers (each containing 4 Mg atoms) and a vacuum thickness of 10 Å. The topmost three atomic layers were allowed to relax, while the bottom two were held fixed to the positions of bulk Mg. Calculations were performed using 2×2 surface unit cells, with $9 \times 9 \times 1$ **k**-point grids and replacing one of the four surface Mg atoms by one 3*d* (Sc, Cr, Mn, Zn), 4*d* (Y, Nb, Mo, Tc, Cd) or 5*d* (Lu, Hf, Ta, W, Re, Os, Ir, Pt, Au, Hg) TM atom (i.e., 19 Mg atoms plus 1 TM in total in the system). These settings have been extensively tested in our previous works.

Table 1
List of preferential adsorption sites on the Mg(0001) surface for all the 3*d*, 4*d*, and 5*d* TMs from our investigations (B = bridge, T = top, Hfcc = hollow-fcc, and Hhcp = hollow-hcp).

3*d* TMs	Sc	Ti[a]	V[b]	Cr	Mn	Fe[b]	Co[b]	Ni[a]	Cu[b]	Zn
adsorption site	B	B	B	Hhcp	B	B	B	B	Hfcc	Hfcc
4*d* TMs	Y	Zr[b]	Nb	Mo	Tc	Ru[b]	Rh[b]	Pd[b]	Ag[b]	Cd
adsorption site	T	T	T	B	B	B	B	B	Hfcc	Hfcc
5*d* TMs	Lu	Hf	Ta	W	Re	Os	Ir	Pt	Au	Hg
adsorption site	B	T	T	B	B	B	B	B	Hfcc	Hfcc

[a] Ref. [8].
[b] Ref. [9].

Adsorption preferences for all TMs on the Mg(0001) surface were checked in four possible sites (top, bridge, hollow-fcc and hollow-hcp). Preference for substitution inside one of the first three layers of bulk Mg, rather than on surface, was determined by comparing E(19 Mg + 1 TM) + E(1 Mg) [i.e., the total energy of the system with one TM substituting one Mg atom in a layer, plus the energy of one Mg atom in the bulk] with the total energy of the system, E(20 Mg + 1 TM), where a TM has been added on surface.

A hydrogen molecule was located on top a TM at a distance of 5 Å for each TM-doped Mg(0001) surface and allowed to relax (this would represent the initial state for energy barrier calculations) in order to find the projected density of states (PDOS) for the TM-doped Mg surfaces.

The position of the *d*-band centre for the TMs used as dopants of the Mg(0001) surfaces was then calculated. The *d*-band centre is defined as the first energy moment of the *d*-band $p_d(E)$ (which is defined as the projection of the electronic density of states onto *d* type spherical harmonics). The position of the *d*-band centre of a TM with respect to the Fermi energy E_F is given by $E_d = \int_{-\infty}^{E_0} dE(E - E_F)p_d(E)$, where E_0 is some cutoff energy which we chose to be 7 eV above the Fermi energy, as in our previous work.

The figures for the individual TM adsorption sites were made using the VMD software [22], whereas those for the PDOS were made using the Xmgr plotting tool [23].

3. Results

3.1. TMs on-surface and layer substitutional preferences

As mentioned in the Introduction, in our previous works we have studied most of 3*d* and 4*d* TMs. Here we wanted to: complete all 3*d* TMs investigating Sc, Cr, Mn and Zn; finish all 4*d* TMs investigating Y, Nb, Mo, Tc, and Cd; study all 5*d* TMs investigating Lu, Hf, Ta, W, Re, Os, Ir, Pt, Au, and Hg (with Lu and Hg never studied so far in literature).

We were interested in on-surface preferential sites for all TMs adsorbed on the Mg(0001) surface. In addition, we now aimed to look also at the substitutional preferences for all the TMs under investigation (i.e., from Sc to Hg), with individual TMs substituted in the first, second or third layer.

As mentioned in Section 2, adsorption preferences for all TMs on the Mg(0001) surface were determined in four possible sites, i.e., top, bridge, hollow-hcp and hollow-fcc (see Fig. 1). The preferred adsorption sites for the TMs here investigated are listed in Table 1. It is interesting to note that the majority of the TMs – Sc, Ti, V, Mn, Fe, Co, Ni, Mo, Tc, Ru, Rh, Pd, Lu, W, Re, Os, Ir and Pt – prefer to adsorb on a bridge site on the Mg(0001) surface. Y, Zr, Nb, Hf and Ta prefer the top site. Cu, Zn, Ag, Cd, Au and Hg prefer the hollow-fcc instead. Cr is the only TM preferring to adsorb on a hollow-hcp.

Tables 2 to 4 list all the information for the 3*d*, 4*d*, and 5*d* TMs respectively, including valence electrons and core radii of the PAW potentials, and the energy difference between the system with the TM substituted in the *n*-th layer and that with the TM adsorbed on the surface, defined by:

$$\Delta E(n) = E(19\ \mathrm{Mg} + 1\ \mathrm{TM}) + E(1\ \mathrm{Mg}) - E(20\ \mathrm{Mg} + 1\ \mathrm{TM}) \quad (1)$$

We recall here that in the past only Wang et al. [15] considered substitution in the first three layers for all 3*d*, 4*d* and 5*d* TMs (although they did not include Lu and Hg), but they substituted after moving a Mg atom to the surface (possibly in the most favourable adsorption site) not removing it from the system, so we will not make a comparison with their results. Chen et al. [13,14] and Tang et al. [16], although proceeded like us by replacing one Mg atom with a TM atom, studied only first and second layer substitutions.

Here we have studied all 3*d*, 4*d* and 5*d* TMs and substituted them in the first, second, and third layer. We find that only Cr, besides Fe, needs spin-polarised calculations (although Co is magnetic too, we previously showed that it can be treated as non-magnetic when used as dopant of the Mg surface). Infact, non-magnetic calculations for Cr on-surface adsorption would give significantly different slab energy values (of about 2.5 eV) from spin-polarised ones.

We find that the majority of the TMs follow the substitutional trend previously observed by Chen et al. [13,14] and Tang et al. [16]. Besides Cd, we also find Hg (not studied before) to prefer a first layer substitution. In addition, we also find that Co, Zn, Ru, Rh, Lu and Au prefer to substitute deeper, in the third layer, instead of the second one found by Chen et al. and Tang et al. who did not consider investigating third layer substitutions.

Table 2
List of all the 3*d* TMs we have investigated (those elements from our previous work have been labelled). For each element we report: the electrons treated as valence (VE) and the core radius (r_{core}); the energy difference $\Delta E(n) = E$(19 Mg + 1 TM) + E(1 Mg) - E(20 Mg + 1 TM) between TM substituted in the first (n = 1), second (n = 2) or third (n = 3) layer and TM adsorbed on surface. The lowest energy, corresponding to the preferred substitutional layer, is highlighted in bold.

3*d* TMs	VE, r_{core} (Å)	ΔE(1) (eV)	ΔE(2) (eV)	ΔE(3) (eV)
Sc	$3s^2 3p^6 3d^1 4s^2$, 1.3	−3.206	**−3.662**	−3.604
Ti[a]	$3d^2 4s^2$, 1.5	−3.526	**−4.286**	−4.216
V[a]	$3s^2 3p^6 3d^3 4s^2$, 1.2	−3.606	**−4.437**	−4.355
Cr	$3p^6 3d^5 4s^1$, 1.2	−1.005	**−1.711**	−1.653
Mn	$3d^5 4s^2$, 1.2	−3.307	**−3.883**	−3.854
Fe[a]	$3d^6 4s^2$, 1.2	−2.700	**−3.056**	−3.018
Co[a]	$3d^7 4s^2$, 1.2	−2.725	−3.067	**−3.073**
Ni[a]	$3d^8 4s^2$, 1.2	−2.436	**−2.658**	−2.625
Cu[a]	$3d^{10} 4s^1$, 1.2	−2.190	**−2.302**	−2.289
Zn	$3d^{10} 4s^2$, 1.2	−2.228	−2.272	**−2.290**

[a] These elements were studied in Ref. [9] considering only first layer substitution.

Table 3
List of all the 4*d* TMs we have investigated (those elements from our previous work have been labelled). For each element we report: the electrons treated as valence (VE) and the core radius (r_{core}); the energy difference $\Delta E(n) = E$(19 Mg + 1 TM) + E(1 Mg) - E(20 Mg + 1 TM) between TM substituted in the first (n = 1), second (n = 2) or third (n = 3) layer and TM adsorbed on surface. The lowest energy, corresponding to the preferred substitutional layer, is highlighted in bold.

4*d* TMs	VE, r_{core} (Å)	ΔE(1) (eV)	ΔE(2) (eV)	ΔE(3) (eV)
Y	$4s^2 4p^6 4d^1 5s^2$, 1.4	−2.971	**−3.336**	−3.208
Zr[a]	$4s^2 4p^6 4d^2 5s^2$, 1.3	−3.778	**−4.700**	−4.597
Nb	$4s^2 4p^6 4d^4 5s^1$, 1.2	−4.142	**−5.266**	−5.158
Mo	$4d^5 5s^1$, 1.5	−4.145	**−5.168**	−5.089
Tc	$4p^6 4d^5 5s^2$, 1.3	−3.862	**−4.674**	−4.661
Ru[a]	$4d^7 5s^1$, 1.4	−3.379	−4.021	**−4.051**
Rh[a]	$4d^8 5s^1$, 1.3	−2.879	−3.309	**−3.338**
Pd[a]	$4d^{10}$, 1.3	−2.490	**−2.702**	−2.694
Ag[a]	$4d^{10} 5s^1$, 1.3	−2.244	**−2.335**	−2.333
Cd	$4d^{10} 5s^2$, 1.2	**−2.244**	−2.202	−2.224

[a] These elements were studied in Ref. [9] considering only first layer substitution.

Table 4
List of all the 5*d* TMs we have investigated. For each element we report: the electrons treated as valence (VE) and the core radius (r_{core}); the energy difference $\Delta E(n) = E(19\ Mg + 1\ TM) + E(1\ Mg) - E(20\ Mg + 1\ TM)$ between TM substituted in the first (n = 1), second (n = 2) or third (n = 3) layer and TM adsorbed on surface. The lowest energy, corresponding to the preferred substitutional layer, is highlighted in bold.

5*d* TMs	VE, r_{core} (Å)	$\Delta E(1)$ (eV)	$\Delta E(2)$ (eV)	$\Delta E(3)$ (eV)
Lu	$5p^6 5d^1 6s^2$, 1.6	−2.972	−3.945	**−3.983**
Hf	$5p^6 5d^2 6s^2$, 1.4	−3.872	**−4.812**	−4.724
Ta	$5d^3 6s^2$, 1.5	−4.320	**−5.511**	−5.407
W	$5d^4 6s^2$, 1.5	−4.432	**−5.587**	−5.487
Re	$5d^5 6s^2$, 1.4	−4.199	**−5.180**	−5.119
Os	$5d^6 6s^2$, 1.4	−3.673	**−4.513**	−4.490
Ir	$5d^7 6s^2$, 1.4	−3.097	**−3.735**	−3.710
Pt	$5d^9 6s^1$, 1.3	−2.620	**−2.970**	−2.923
Au	$5d^{10} 6s^1$, 1.3	−2.293	−2.410	**−2.412**
Hg	$5d^{10} 6s^2$, 1.3	**−2.037**	−1.964	−1.994

Table 5
List of 3*d*, 4*d*, and 5*d* TMs with their corresponding *d*-band centre positions, referred to the Fermi energy, found in our investigations.

3*d* TMs	Sc	Ti[a]	V[a]	Cr	Mn	Fe[a]	Co[a]	Ni[a]	Cu[a]	Zn
d-band (eV)	1.66	1.08	0.82	0.52	0.28	−0.72	−0.16	−0.79	−2.27	−6.73
4*d* TMs	Y	Zr[a]	Nb	Mo	Tc	Ru[a]	Rh[a]	Pd[a]	Ag[a]	Cd
d-band (eV)	1.90	1.32	1.10	0.64	0.24	−0.14	−0.75	−1.84	−4.14	−8.15
5*d* TMs	Lu	Hf	Ta	W	Re	Os	Ir	Pt	Au	Hg
d-band (eV)	2.21	1.51	1.18	0.77	0.37	−0.09	−0.67	−1.88	−3.67	−6.59

[a] Ref. [9].

3.2. *d*-band centre positions

The *d*-band centre results for all the 3*d* to 5*d* TMs we have investigated are shown in Table 5. These have been calculated placing the TMs in the first-layer to compare the present results with those we previously reported for Ni and Ti (Ref. [8]).

Looking at the general trend, we can see that the *d*-band centre values are positive for the elements at the left of the Periodic Table, whereas they get smaller and reach quite negative values moving to the right of the Periodic Table. All *d*-band centre values are also plotted in Fig. 2 as a function of the atomic number, where the trend is clearly visible for the 3*d* (filled black circles), 4*d* (filled red circles) and 5*d* (filled green circles) TMs respectively.

Out of all these results, we find that Fe, Ni and Rh remain the most active catalysts, as we previously suggested.

Finally, we have also calculated the PDOS for H_2 dissociating over all the TM-doped Mg surfaces investigated (with the TMs substituting in the first layer). In particular, Figs. 3–5 show the PDOS for Mg surfaces doped with Zn, Tc and Lu respectively. These were chosen as an example of very negative, almost null and very positive *d*-band centre value, respectively. Zn is a late 3*d* TM with all the *d* orbitals filled, Tc is a mid 4*d* TM with the *d* orbitals half filled, whereas Lu is an early 5*d* TM with almost empty (only one electron) *d* orbitals. This means that Lu has a higher reactivity than both Tc and Zn, and its *d*-band centre position is infact much higher than that of the other two TMs (as per values reported in Table 5). This suggests that molecular hydrogen dissociation on a Lu-doped Mg surface would display an energy barrier lower than that for a Tc- or Zn-doped Mg surfaces, however, as discussed above, the corresponding *d*-band value is much more positive than the ideal value of −1.29 eV, and therefore we would expect a very high barrier for hydrogen diffusion.

Figs. 6–8 show the PDOS for Mg surfaces doped with the most active catalysts we have identified, i.e., Rh, Ni and Fe respectively. These elements have almost full *d* orbitals and known to give small energy barriers for both hydrogen dissociation and diffusion (Ref. [9]).

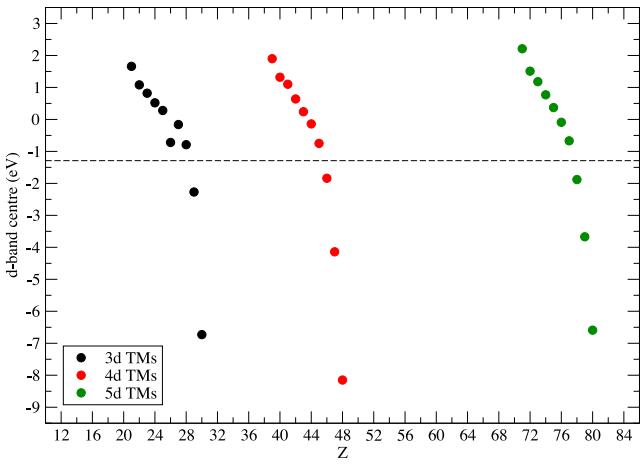

Fig. 2. Plot of *d*-band centre values, referred to the Fermi energy, as a function of the atomic number for all 3*d* to 5*d* TMs. The horizontal dashed line marks the ideal value of −1.29 eV as highlighted in our previous work (Ref. [9]). (For interpretation of the references to colour in this figure legend, the reader is referred to the web version of this article.)

4. Conclusions

We have carried out a systematic DFT investigation of hydrogen sorption properties on 3*d*, 4*d* and 5*d* TM-doped Mg(0001) surfaces, by including all the TMs we did not investigate in our previous works [8, 9].

We have studied substitutional preferences in different layer locations (i.e., first, second and third layer of bulk Mg) and compared the results with those previously presented in literature for several of them. We find that the majority of the TMs prefer to substitute in the second layer, apart from Cd and Hg which prefer first layer substitution, whereas Co, Zn, Ru, Rh, Lu and Au prefer third layer substitution instead.

Here we have also presented a complete list of *d*-band centre positions values for all 3*d*, 4*d* and 5*d* TMs of the Periodic Table in search for the possible ideal TM for hydrogen storage purposes. Our results show that the most active catalysts for the relevant reactions involved in the hydrogen storage properties of doped Mg are Fe, Ni and Rh, which are also those with their *d*-band centres closer to the ideal value of −1.29 eV.

CRediT authorship contribution statement

M. Pozzo: Writing – review & editing, Writing – original draft, Visualization, Validation, Resources, Methodology, Investigation, Formal analysis, Data curation, Conceptualization. **D. Alfè:** Writing – review & editing, Resources, Project administration, Funding acquisition.

Declaration of competing interest

The authors declare that they have no known competing financial interests or personal relationships that could have appeared to influence the work reported in this paper.

Acknowledgements

M.P. and D.A. acknowledge MUR for the support of the PRIN Project no. 20222FXZ33 entitled “Materials modelling for energy storage applications”. Calculations were performed on the Monsoon2 system (a collaborative facility supplied under the Joint Weather and Climate Research Programme, a strategic partnership between the UK Met Office and the Natural Environment Research Council), and on the computational infrastructure of Upper Lazio Science and Technology Park (Rieti, Italy).

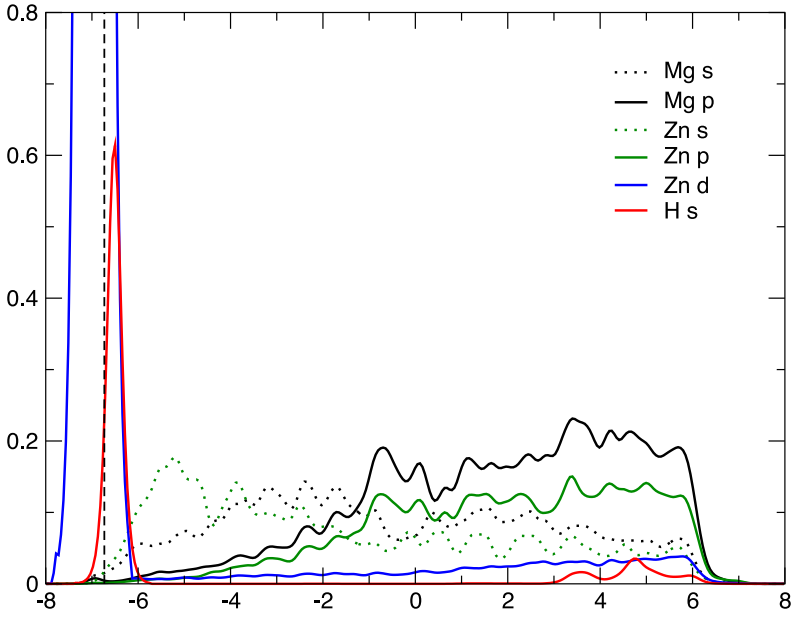

Fig. 3. Projected density of states for molecular hydrogen approaching a Zn-doped Mg surface for dissociation, as a function of the energy relative to the Fermi level. The position of the *d*-band centre is shown as a dashed vertical line.

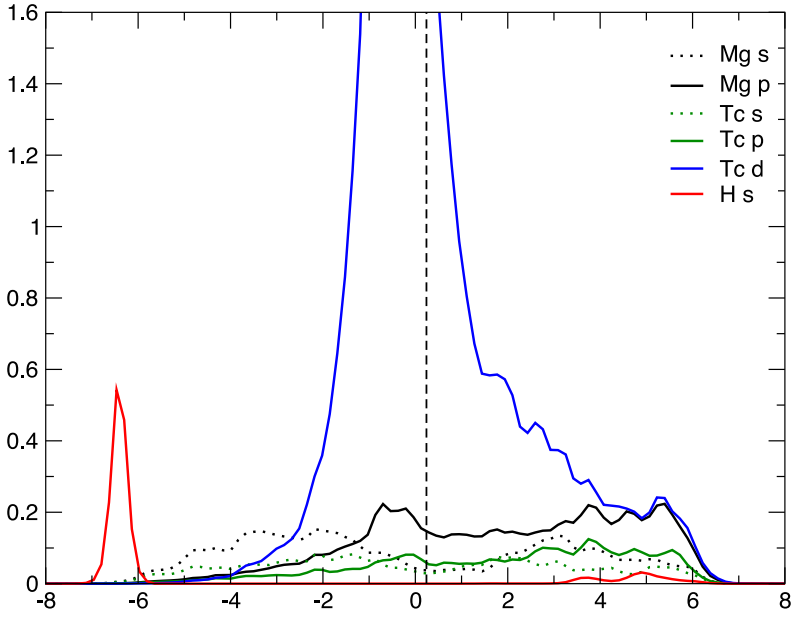

Fig. 4. Projected density of states for molecular hydrogen approaching a Tc-doped Mg surface for dissociation, as a function of the energy relative to the Fermi level. The position of the *d*-band centre is shown as a dashed vertical line.

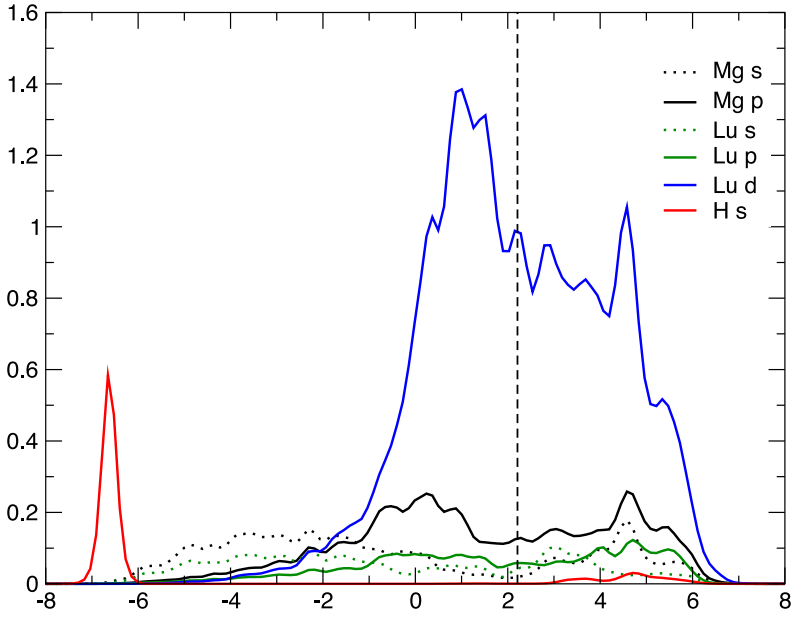

Fig. 5. Projected density of states for molecular hydrogen approaching a Lu-doped Mg surface for dissociation, as a function of the energy relative to the Fermi level. The position of the *d*-band centre is shown as a dashed vertical line.

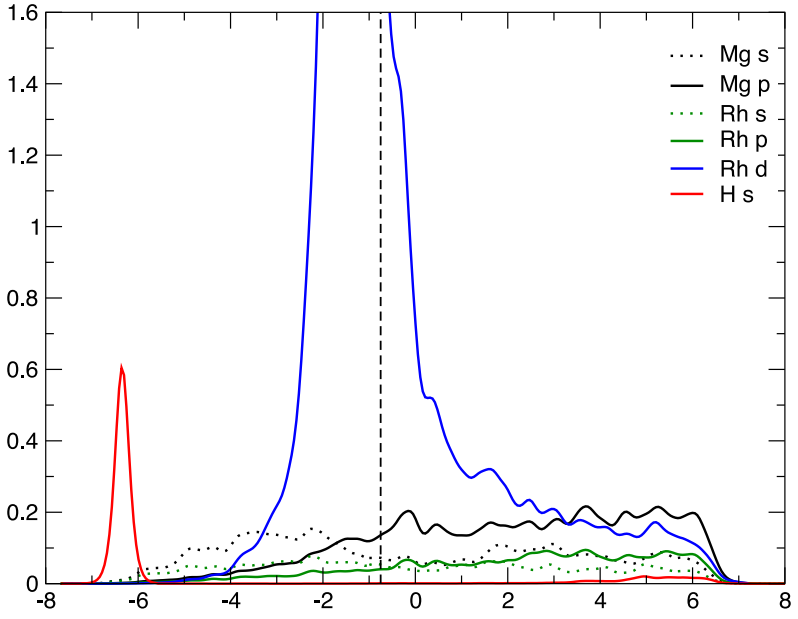

Fig. 6. Projected density of states for molecular hydrogen approaching a Rh-doped Mg surface for dissociation, as a function of the energy relative to the Fermi level. The position of the *d*-band centre is shown as a dashed vertical line.

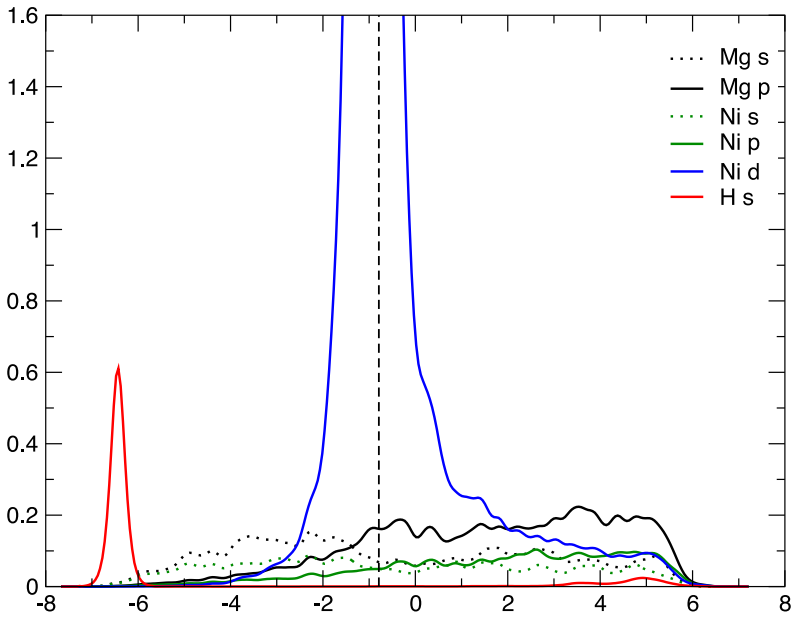

Fig. 7. Projected density of states for molecular hydrogen approaching a Ni-doped Mg surface for dissociation, as a function of the energy relative to the Fermi level. The position of the *d*-band centre is shown as a dashed vertical line.

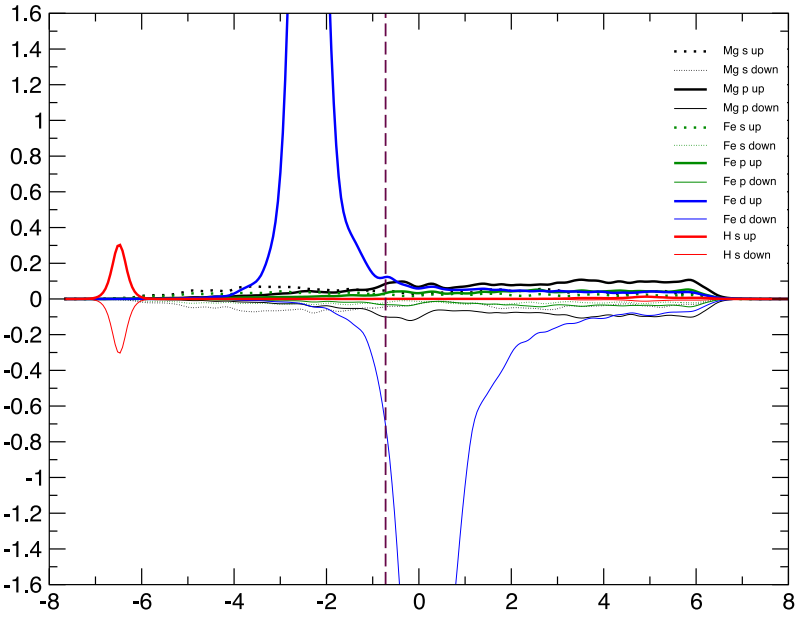

Fig. 8. Projected density of states for molecular hydrogen approaching a Fe-doped Mg surface for dissociation, as a function of the energy relative to the Fermi level, from spin-polarised calculations (spin-down PDOS are plotted specularly with respect to the corresponding spin-up PDOS). The position of the *d*-band centre is shown as a dashed vertical line.

References

[1] Møller KT, Jensen RT, Akiba E, Li H-W. Hydrogen - A sustainable energy carrier. Prog Nat Sci Mater Int 2017;27:34.

[2] Shao H, He L, Lin H, Li H-W. Progress and Trends in Magnesium-Based Materials for Energy-Storage Research: A Review. Energy Technol 2018;6:445.

[3] Sun Y, Shen C, Lai Q, Liu W, Wang D-W, Aguey-Zinsou K-F. Tailoring magnesium based materials for hydrogen storage through synthesis: Current state of the art. Energy Storage Mater 2018;10:168.

[4] Abe JO, Popoola API, Ajenifuja E, Popoola OM. Hydrogen energy, economy and storage: Review and recommendation. Int J Hydrog Energy 2019;44:15072.

[5] Yang X, Lu X, Zhang J, Hou Q, Zou J. Progress in improving hydrogen storage properties of Mg-based materials. Mater Today Adv 2023;19:100387.

[6] Hong H, Harrison ARP, Nie B. Linking the microstructure of ball-milled Mg-Ni hydrogen storage materials to reactive properties and techno-economic feasibility. Energy Fuels 2025;39:13789.

[7] Borchloo A, Nekouee K. A review of enhanced hydrogen storage in MgH_2: the role of high-energy reactive ball milling and catalysis. Synth Sinter 2025;5:200.

[8] Pozzo M, Alfè D, Amieiro A, French S, Pratt A. Hydrogen dissociation and diffusion on Ni- and Ti-doped Mg(0001) surfaces. J Chem Phys 2008;128:094703.

[9] Pozzo M, Alfè D. Hydrogen dissociation and diffusion on transition metal(=Ti, Zr, V, Fe, Ru, Co, Rh, Ni, Pd, Cu, Ag)-doped Mg(0001) surfaces. Int J Hydrog Energy 2009;34:1922.

[10] Hammer B, Nørskov JK. Electronic factors determining the reactivity of metal surfaces. Surf Sci 1995;343:211.

[11] Banerjee S, Pillai CGS, Majumder C. First-principles study of the H_2 interaction with transition metal (Ti, V, Ni) doped Mg(0001) surface: Implications for H-storage materials. J Chem Phys 2008;129:174703.

[12] Wu G, Zhang J, Wu Y, Li Q, Chou K, Bao X. The effect of defects on the hydrogenation in Mg(0001) surface. Appl Surf Sci 2009;256:46.

[13] Chen M, Yang X-B, Cui J, Tang J-J, Gan L-Y, Zhu M, Zhao Y-J. Stability of transition metals on Mg(0001) surfaces and their effects on hydrogen adsorption. Int J Hydrog Energy 2012;37:309.
[14] Chen M, Cai Z-Z, Yang X-B, Zhu M, Zhao Y-J. Theoretical study of hydrogen dissociation and diffusion on Nb and Ni co-doped Mg(0001): A synergistic effect. 606, 2012, p. 145,
[15] Wang Z, Guo X, Wu M, Sun Q, Jia Y. First-principles study of hydrogen dissociation and diffusion on transition metal-doped Mg(0001) surfaces. Appl Surf Sci 2014;305:40.
[16] Tang J-J, Yea J-H, Fang Y-X, Lin Z, Zhao Y-J. Transition metal substitution on Mg(10$\bar{1}$3) and Mg(0001) surfaces for improved hydrogenation and dehydrogenation: A systematic first-principles study. Appl Surfcae Sci 2019;479:626.
[17] Han Z, Wu Y, Yu H, Zhou S. Location-dependent effect of nickel on hydrogen dissociation and diffusion on Mg (0001) surface: Insights into hydrogen storage material design. J Magnes Alloy 2022;10:1617.
[18] Kresse G, Furthmüller J. Efficient iterative schemes for ab initio total-energy calculations using a plane-wave basis set. Phys Rev B 1996;54:11169.
[19] Blöchl PE. Projector augmented-wave method. Phys Rev B 1994;50:17953.
[20] Kresse G, Joubert J. From ultrasoft pseudopotentials to the projector augmented-wave method. Phys Rev B 1999;59:1758.
[21] Perdew JP, Burke K, Ernzerhof M. Generalized gradient approximation made simple. Phys Rev Lett 1996;77:3865.
[22] Humphrey W, Dalke A, Schulten K. VMD: visual molecular dynamics. J Mol Graph 1996;14:33.
[23] Copyright (c) 1991-95 P.J. Turner, Portland.